Electromagnetic draping of merging neutron stars

Maxim Lyutikov

Department of Physics and Astronomy, Purdue University, 525 Northwestern Avenue, West Lafayette, Indiana 47907-2036, USA

We first derive a set of equations describing general stationary configurations of relativistic force-free plasma, without assuming any geometric symmetries. We then demonstrate that electromagnetic interaction of merging neutron stars is necessarily dissipative due to the effect of electromagnetic draping—creation of dissipative regions near the star (in the single magnetized case) or at the magnetospheric boundary (in the double magnetized case). Our results indicate that even in the single magnetized case we expect that relativistic jets (or "tongues") are produced, with correspondingly beamed emission pattern.

I. INTRODUCTION

The detection of gravitational waves associated with a short GRB [1] identifies merger of neutron stars as the central engine. It is highly desirable to detect any possible precursor to the main event. Reference [2] (see also Ref. [3]) argued that magnetospheric interaction during double neutron star (DNS) merger can lead to the production of electromagnetic radiation. The underlying mechanism advocated in those works is a creation of inductive electric field due to the relative motion of neutron stars. Both singly magnetized (1M-DNS) and double magnetized case (2M-DNS) are possible [4]. The 1M-DNS case is similar to the Io-Jupiter interaction [5]. Other relevant works include Refs. [6–8].

Similarly to the DNS merger, in the case of merging black holes, or BH-NS mergers, motion of the black hole through magnetic field (generated ether by the accretion disk or through neutron star magnetosphere) leads to generation of inductively-induced outflows, even by a nonrotating Schwarzschild black hole [9–12].

In the present work we make an important step in extending the work of Refs. [2,4] to include the ideal plasma constraint right from the beginning. The approach taken by Refs. [2,4], heuristically, follows that of Ref. [13], in that a quasivacuum approximation is used at first. This leads to the generation of dissipative regions, pair production, and ensuing nearly ideal plasma dynamics. Resulting charges and currents modify the magnetospheric structure.

In the classical pulsar problem, one starts with the ideal plasma constraint right from the beginning: in the axisymmetric case this then leads to the pulsar equation [14,15]. The pulsar equation, a variant of the Grad-Shafranov equation [16,17], is a scalar equation for axially-symmetric relativistic force-free configurations. Axial symmetry allows introduction of an associated Euler potential which, together with the div **B** = 0 and ideal conditions, reduce the force balance to a single scalar equation.

This is the step accomplished in the present paper for the case of linear motion of a conducting sphere through force-free magnetic fields: instead of starting with vacuum-like configurations and finding the $\mathbf{E} \cdot \mathbf{B} \neq 0$ regions, the condition $\mathbf{E} \cdot \mathbf{B} = 0$ is imposed from the beginning. This immediately takes the effects of the induced charges and currents on the global structure of the magnetic field.

In the case of merger double neutron stars systems, there is no geometrical symmetry that can be used to reduce the force balance to a single equation. In this paper we first derive equation governing relativistic force-free configurations *without assuming axially symmetry* in Sec. II. It is a set of two nonlinear elliptic equations for two Euler potential, with initially unknown dependence of the electric potential. It turns out to be prohibitively complicated.

In Sec. III we take an alternative approach: expansion in small electric field (small velocity). We demonstrate that the electromagnetic fields "pile up" near the surface of the neutron star, creating regions with large electric field. Similar effects occur in 2M-DNS scenario in Sec. IV.

II. RELATIVISTIC FORCE-FREE CONFIGURATIONS

First we derive a set of equations describing general stationary configurations of relativistic force-free plasma, without assuming any geometric symmetries.

A convenient way to represent the magnetic field is in terms of Euler potentials $\alpha - \beta$ (e.g., Ref. [18]):

$$\mathbf{B} = \nabla\alpha \times \nabla\beta. \tag{1}$$

Two scalar function α and β are conserved along field lines. In addition, stationary electric field can be represented in terms of the electrostatic potential Φ (factors of 4π are absorbed into definitions of fields):

$$\mathbf{E} = -\nabla\Phi. \tag{2}$$

The Ideal condition

$$\mathbf{E} \cdot \mathbf{B} = \nabla\Phi \cdot (\nabla\alpha \times \nabla\beta) \tag{3}$$

then requires $\Phi(\alpha)$ or $\Phi(\beta)$. For definiteness let us assume $\Phi(\alpha)$. This is an initially unknown function that needs to be found as part of the solution with given boundary conditions.

025205-1

Also, we impose orthogonality condition

$$(\nabla\alpha \cdot \nabla\beta) = 0. \tag{4}$$

Then vectors $\nabla\alpha$, $\nabla\beta$, and $\nabla\Phi$ form an orthogonal triad. Surfaces of constant α, β, Φ are mutually orthogonal.

Force balance

$$\Delta\Phi\nabla\Phi + (\nabla \times \mathbf{B}) \times \mathbf{B} = 0 \tag{5}$$

takes the form

$$\nabla\beta(\nabla\alpha \cdot (-\nabla\alpha\Delta\beta + \mathcal{L}(\alpha, \beta))) + \nabla\alpha((\nabla\alpha \cdot \nabla\alpha)\Phi'\Phi''$$
$$+ \Delta\alpha(\Phi')^2 - (\nabla\beta \cdot (\mathcal{L}(\alpha, \beta) + \Delta\alpha\nabla\beta))) = 0, \tag{6}$$

where

$$\mathcal{L}(\alpha, \beta) \equiv (\nabla\alpha \cdot \nabla)\nabla\beta - (\nabla\beta \cdot \nabla)\nabla\alpha, \tag{7}$$

and primes denote $\Phi' = \partial_\alpha \Phi(\alpha)$.

Both terms in Eq. (6) should be zero independently:

$$\nabla\alpha \cdot (-\nabla\alpha\Delta\beta + \mathcal{L}(\alpha, \beta)) \tag{8}$$

$$(\nabla\alpha)^2\Phi'\Phi'' + \Delta\alpha(\Phi')^2 = (\nabla\beta \cdot (\mathcal{L}(\alpha, \beta) + \Delta\alpha\nabla\beta)). \tag{9}$$

Equations (8) and (9), together with constraint Eq. (4) represent two equations for two Euler potentials α and β.

The system of equations [Eqs. (4), (8), and (9)] generalizes the famous Grad-Shafranov equation [16,17]—in fact, its relativistic generalization [14,15]—to arbitrary, not necessarily axially symmetric, configuration. Two steps are required to recover the (relativistic) Grad-Shafranov: (i) one Euler potential is assumed $\beta = \phi$, the toroidal coordinate; (ii) the magnetic field is then chosen as $\mathbf{B} = (\nabla\alpha) \times (\nabla\phi) + f(\alpha)(\nabla\phi)$ with $f(\alpha)$ is some function, to be found together with the solution.

In the case of Grad-Shafranov equation, the divergence-free condition, ideal condition and assumption of axial symmetry reduce the force balance to a single scalar equation. In our case, the axial symmetry is dropped: potential β needs to be determined independently, hence there are two equations to be solved.

Similar to the original Grad-Shafranov, where the dependence of the poloidal current [incorporated into function] needs to be found together with the solution α, in our case for given boundary conditions, dependence of $\Phi(\alpha)$ should be found together with solutions for two functions α and β. Generally, this will involve an elliptic relaxation scheme for two nonlinearly coupled equations for α and β and dependence of $\Phi(\alpha)$. It's a mathematically complicated procedure, but the problem is well formulated.

Some further modifications can be done. Equation (8) can be written as

$$\nabla\alpha\Delta\beta = \mathcal{L}(\alpha, \beta) + g\nabla\beta, \tag{10}$$

where g is an arbitrary function. Scalar product in Eq. (10) with $\nabla\beta$ gives

$$(\nabla\beta \cdot \mathcal{L}(\alpha, \beta)) = -g(\nabla\beta \cdot \nabla\beta). \tag{11}$$

Equation (9) then becomes

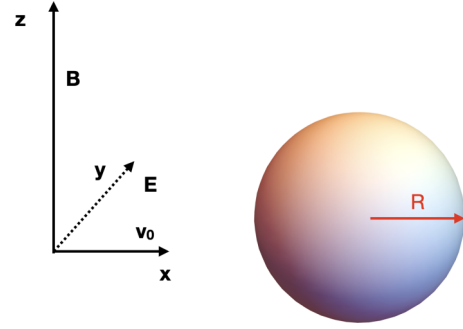$$(\nabla\alpha)^2\Phi'\Phi'' + \Delta\alpha(\Phi')^2 = (\nabla\beta)^2(\Delta\alpha - g) = 0 \tag{12}$$

FIG. 1. Geometry of the system. In the frame of the sphere at large $x \to -\infty$ the magnetic field is along z axis, electric field is along y axis, so that plasma is moving in positive z direction with velocity v_0.

or

$$\Delta\alpha((\Phi')^2 - (\nabla\beta)^2) + (\nabla\alpha)^2\Phi'\Phi'' + g(\nabla\beta)^2 = 0. \tag{13}$$

Equations (10) and (13) can be used instead of Eqs. (8) and (9). Function g should be chosen to fit the boundary conditions.

The set of Eqs. (8), (9), and (4) or (10), (13), and (4) describe a general type of relativistic force-free equilibrium. It is a nonlinear set of equations for two functions α and β with initially unknown $\Phi(\alpha)$.

III. METAL SPHERE MOVING THROUGH FORCE-FREE MAGNETIC FIELD

A. Boundary conditions

LIn the frame of a conducting ball the magnetic field at infinity is along z axis and electric field is along y axis (so that electromagnetic velocity is along x), see Fig. 1. The magnetic field is assumed to be nonpenetrating, the ball is unmagnetized.

A set of equations that needs to be solved is:

$$\rho_e\mathbf{E} + \mathbf{J} \times \mathbf{B} = 0,$$
$$\text{div}\,\mathbf{J} = 0,$$
$$\mathbf{E} \cdot \mathbf{B} = 0, \tag{14}$$

force balance, stationarity and ideality. Boundary conditions are:

$$B_z(x = -\infty) = B_0,$$
$$E_y(x = -\infty) = v_0 B_z,$$
$$\mathbf{e}_r \cdot \mathbf{B}|_{r=R} = 0,$$
$$\mathbf{e}_r \times \mathbf{E}|_{r=R} = 0. \tag{15}$$

The last two imply no normal magnetic field and no tangential electric field on the surface.

There is a natural freedom in choosing the vector potential for the magnetic field. First, for stationary configurations the Coulomb gauge $\nabla \cdot \mathbf{A}$ is preferred. Next, two types of Coulomb-type gauges are commonly used, the symmetric and the Landau gauge (e.g., Ref. [19], paragraph 112 and the accompanying problem). In our case the Landau gauge for

magnetic field is better at $x = \infty$). In terms of Euler potentials we find then:

$$\beta(x = -\infty) = -x,$$
$$\alpha(x = -\infty) = B_0 y,$$
$$\mathbf{e}_r \cdot (\nabla\alpha \times \nabla\beta)|_{r=R} = 0,$$
$$\mathbf{e}_r \times \nabla\alpha|_{r=R} = 0. \qquad (16)$$

Thus, in Landau gauge at $x = -\infty$ we have $\Phi = -v_0 B_0 y = -v_0 \alpha$.

The resulting system of nonlinear elliptical equations with unknown $\Phi(\alpha)$ turns out to be prohibitively complicated, hence we have to resort to approximate methods—expansion in terms of the velocity v_0.

B. Metal ball in static magnetic field, $v_0 = 0$

As a zeroth order, we start with conducting ball in external magnetic field. In this case magnetic field and vector potential are a sum of constant vertical field $\mathbf{B}_v$ and dipole field $\mathbf{B}_d$ (below we use spherical coordinates $\{r, \theta, \phi\}$).

$$\mathbf{B}_0 = \mathbf{B}_v + \mathbf{B}_d = \left\{ (1 - R^3/r^3)\cos\theta, -\left(1 + \frac{R^3}{2r^3}\right) \times \sin\theta, 0 \right\} B_0,$$

$$\mathbf{A} = \{0, 0, 1 - R^3/r^3\} r\sin\theta B_0/2,$$

$$\mathbf{B}_v = \{\cos\theta, -\sin\theta, 0\} B_0,$$

$$\mathbf{B}_d = \left\{ -R^3/r^3 \cos\theta, -\frac{R^3}{2r^3}\sin\theta, 0 \right\} B_0. \qquad (17)$$

Euler potentials are

$$\alpha_0 = \frac{1}{2} B_0 \sin^2\theta \left(r^2 - \frac{R^3}{r} \right),$$
$$\beta_0 = \phi. \qquad (18)$$

Scalar magnetic potential

$$\Phi_B = \left(1 + \frac{R^3}{2r^3}\right) r\cos\theta B_0, \qquad (19)$$

so that $\mathbf{B}_0 = \nabla\alpha_0 \times \nabla\beta_0 = \nabla\Phi_B$.

Importantly,

$$(\nabla\alpha_0) \cdot (\nabla\Phi_B) = 0. \qquad (20)$$

Thus, Euler potentials α_0, β_0, and Φ_0 form a mutually orthogonal triad of surfaces, see Fig. 2,

$$\nabla\alpha_0 \perp \nabla\beta_0 \perp \nabla\Phi_B. \qquad (21)$$

We find

$$\nabla\alpha_0 = \left\{ \left(r + \frac{R^3}{2r^2} \right) \sin^2\theta, \frac{(r^3 - R^3)\sin\theta\cos\theta}{r^2}, 0 \right\} B_0,$$

$$\nabla\beta_0 = \left\{ 0, 0, \frac{1}{r\sin\theta} \right\},$$

$$(\nabla\alpha_0 \cdot \nabla\beta_0) = 0$$

$$\mathcal{L} = \frac{B_0(-4r^3 + 3R^3\cos(2\theta) + R^3)}{2\sin\theta r^4} \mathbf{e}_\phi,$$

$$\mathcal{L} \cdot \nabla\alpha_0 = 0$$

$$\mathcal{L} \cdot \nabla\beta_0 = \frac{B_0(-4r^3 + 3R^3\cos(2\theta) + R^3)}{2\sin^2\theta r^5},$$

$$\Delta\beta_0 = 0,$$

$$(\nabla\beta_0)^2 = \frac{1}{\sin^2\theta r^2},$$

$$(\nabla\alpha_0)^2 = \frac{B_0^2 \sin^2\theta (3R^3\cos(2\theta)(R^3 - 4r^3) - 4r^3 R^3 + 8r^6 + 5R^6)}{8r^4},$$

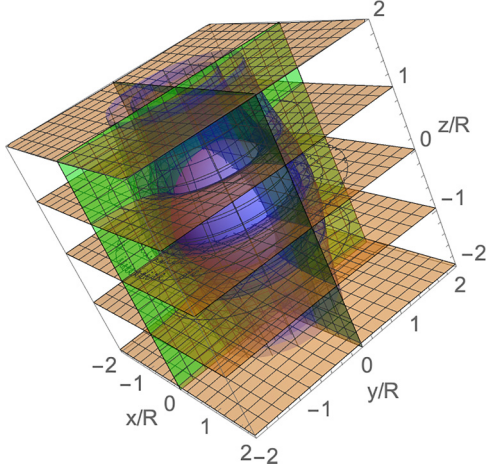$$\Delta\alpha_0 = -\frac{B_0(-4r^3 + 3R^3\cos(2\theta) + R^3)}{2r^3}. \qquad (22)$$

Equation (10) becomes

$$\mathcal{L}(\alpha, \beta) + g_0 \nabla\beta_0 = 0,$$

$$g_0 = \frac{B_0(4r^3 - 3R^3\cos(2\theta) - R^3)}{2r^3}. \qquad (23)$$

For $\Phi = 0$ Eq. (13) becomes

$$g_0 = \Delta\alpha_0, \qquad (24)$$

and it is indeed satisfied.

FIG. 2. Orthogonal surfaces of constant α_0, β_0 and Φ_B.

C. First order expansion in v_0

In Appendix A we demonstrate that in first order expansion in v_0 the surfaces of constant $\alpha - \beta - \Phi$ remain unchanged.

Let us expand the force balance in Eq. (5) for small velocity $v_0 \ll 1$. In the zeroth order

$$\nabla \times \mathbf{B}_0 = 0. \tag{25}$$

We expect that electric potential is first order in v_0

$$\Phi \propto v_0 \sim \frac{E}{B_0},$$
$$\Phi \propto \mathcal{O}(\epsilon). \tag{26}$$

The key point is that the force balance is second order in v_0:

$$\Delta\Phi\nabla\Phi + (\nabla \times \delta\mathbf{B}) \times \mathbf{B}_0 = 0,$$
$$\Delta\Phi\nabla\Phi \propto \mathcal{O}(\epsilon^2),$$
$$(\nabla \times \delta\mathbf{B}) \propto \mathcal{O}(\epsilon^2), \tag{27}$$

while the constraint

$$\mathbf{E} \cdot \mathbf{B} \propto \mathbf{E} \cdot \mathbf{B}_0 \propto \mathcal{O}(\epsilon) \tag{28}$$

is first order. Thus, if we are limited to terms linear in v_0, we need to consider only the constraint: the force balance is violated only in v_0^2.

For magnetic field $\mathbf{B}_0$ let us use the magnetic potential [Eq. (19)]. Then we need to find Φ such that

$$(\nabla\Phi) \cdot (\nabla\Phi_B) = 0. \tag{29}$$

Clearly, any

$$\Phi(\alpha_0)f(\phi) \tag{30}$$

satisfies this condition.

At $x = -\infty$ the electric potential is

$$\Phi = -yv_0B_0 = -r\sin\theta\sin\phi v_0B_0. \tag{31}$$

Thus,

$$\Phi(\alpha_0) = -v_0B_0\sqrt{2\alpha_0},$$
$$f(\phi) = \sin\phi. \tag{32}$$

And finally

$$\Phi = -\sqrt{1 - R^3/r^3} \times r\sin\theta\sin\phi\, v_0B_0,$$

$$\mathbf{E} = -\nabla\Phi = \left\{ \frac{\left(1 + \frac{R^3}{2r^3}\right)}{\sqrt{1 - R^3/r^3}} \sin\theta\sin\phi, \sqrt{1 - R^3/r^3}\cos\theta\sin(\phi), \sqrt{1 - R^3/r^3}\cos\phi \right\} v_0B_0$$

$$\rightarrow \left\{ \frac{\sqrt{3}\sqrt{R}\sin\theta\sin\phi}{2\sqrt{\delta_r}}, \frac{\sqrt{3}\cos\theta\sqrt{\delta_r}\sin\phi}{\sqrt{R}}, \frac{\sqrt{3}\sqrt{\delta_r}\cos\phi}{\sqrt{R}} \right\} v_0B_0.$$

$$\delta_r = r - R. \tag{33}$$

By construction $\mathbf{E} \cdot \mathbf{B}_0 = 0$. The radial component of the electric field diverges—this is the electromagnetic draping. Also, in Appendix B we compare electric field [Eq. (33)] with other relevant cases.

Given the electric field in Eq. (33), the induced charger density is

$$\rho_e = \text{div}\,\mathbf{E} = -\frac{9R^6\sin\theta\sin\phi}{4r^7(1 - R^3/r^3)^{3/2}} B_0 v_0$$
$$\rightarrow -\frac{\sqrt{3}\sqrt{R}\sin\theta\sin\phi}{4\delta_r^{3/2}} B_0 v_0. \tag{34}$$

The electromagnetic velocity is

$$\mathbf{v}_{EM} = \frac{\mathbf{E} \times \mathbf{B}_0}{\mathbf{B}_0^2},$$

$$v_r = \frac{2r^3(2r^3 + R^3)\sqrt{1 - R^3/r^3}}{4(r^3 - R^3)^2 - 3R^3(R^3 - 4r^3)\sin^2\theta}\sin\theta\cos\phi,$$

$$v_\theta = \frac{4r^3(r^3 - R^3)\sqrt{1 - R^3/r^3}}{4(r^3 - R^3)^2 - 3R^3(R^3 - 4r^3)\sin^2\theta}\cos\theta\cos\phi,$$

$$v_\phi = -\frac{\sin\phi}{\sqrt{1 - R^3/r^3}} \rightarrow -\frac{v_0\sin\phi}{\sqrt{3}\sqrt{\delta_r/R}}, \tag{35}$$

see Figs. 3–6.

The condition $\mathbf{v}_{EM} = 1$ is satisfied at approximately

$$\frac{\delta r}{R} = \sin^2\phi\frac{v_0^2}{3}. \tag{36}$$

This is the estimate of the thickness and location of the draping layer. It is maximal at the plane $x = 0$ ($\phi = \pi/2$). In the
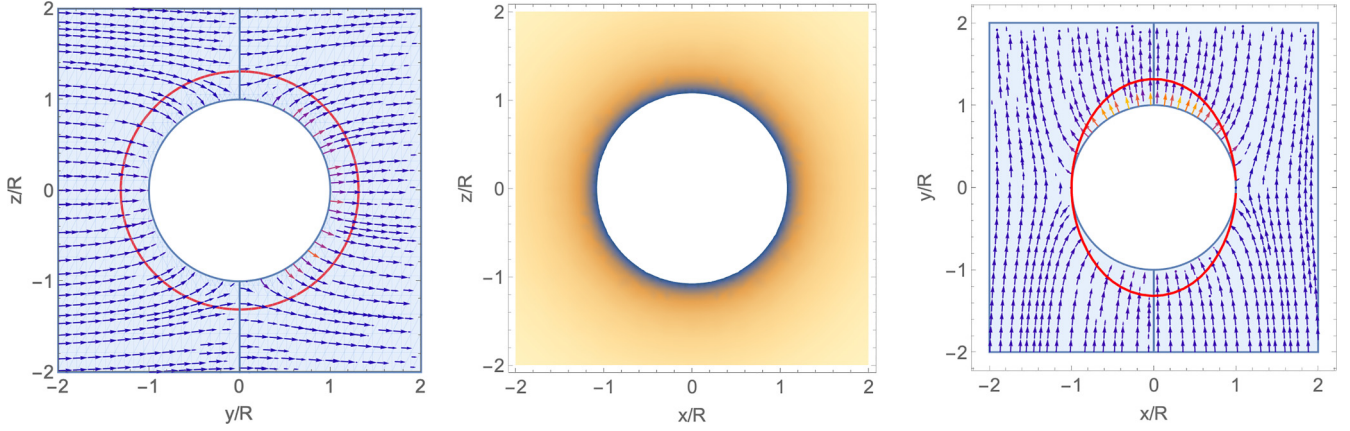
FIG. 3. Electric field [Eq. (33)] in the $x = 0$, $y = 0$, and $z = 0$ planes (for $y = 0$ the electric field is $\sqrt{(x^2 + z^2)^{3/2} - 1}/(x^2 + z^2)^{3/4} \mathbf{e}_y v_0 B_0$). Red lines indicate regions where $\beta_{EM} = 1$ ($v_0 = 0.75$ is assumed for plotting).

$\phi = \pi/2$ plane ($x = 0$) the condition $\beta_{EM} = 1$ is satisfied at

$$\frac{r_{EM}}{R} = \gamma_0^{1/3},$$

$$\gamma_0 = \frac{1}{\sqrt{1 - v_0^2}}. \tag{37}$$

Divergence of the electric field [Eq. (33)] on the surface of the metal sphere moving through force-free field is the key result of the present paper. In the following, Sec. III D, we demonstrate that higher-order effects in v_0 do not resolve the divergence. Thus, our assumption of ideal force-free plasma is violated—the flow *must* become dissipative.
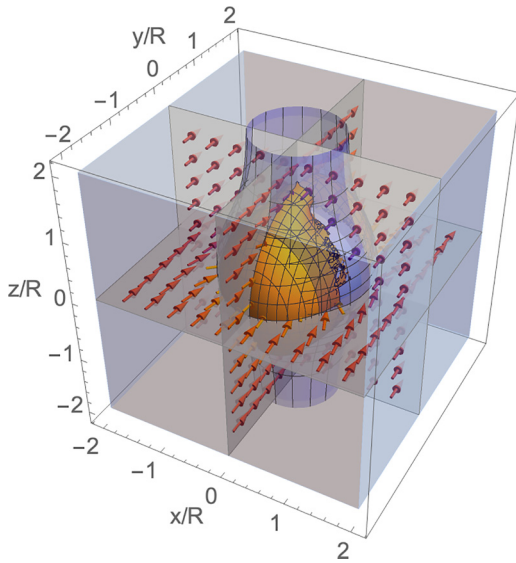

FIG. 4. 3D view of first order electric field [Eq. (33)]. The central sphere is the neutron star. Blue surface is the magnetic field flux surface (magnetic field lines lie on the surface pointing in the z direction. Arrows are electric field sliced at $x = 0, y = 0, z = 0$. In the frame of the neutron star plasma is moving in the $+x$ direction. Bounded earlike surfaces are regions where β_{EM} becomes larger than 1.

D. Second order in v_0

As we discussed above, the first order perturbations come not from the dynamics, but from the constraint $\mathbf{E} \cdot \mathbf{B} = 0$. We can then use the $\propto v_0$ terms to construct the second order expansion.

The charge density [Eq. (34)] and the electromagnetic velocity [Eq. (35)] lead to the appearance of charge-separated current

$$\mathbf{J}_{EM} = \rho_e \mathbf{v}_{EM,} \tag{38}$$

[it is of $\mathcal{O}(\epsilon^2)$ order]. The current $\mathbf{J}_{EM}$ is not the total current, only its transverse charge-separated part, see below. Naturally,

$$\rho_e \mathbf{E} + \mathbf{J}_{EM} \times \mathbf{B}_0 = 0. \tag{39}$$

The most radially divergent ϕ component can be easily found:

$$\mathbf{J}_{\phi}^{(2)} = \frac{9 \sin \theta \sin^2 \phi}{4r(r^3 - R^3)^2} \times R^6 v_0^2 B_0. \tag{40}$$

Near $r \to R$

$$\mathbf{J}_{EM} \approx \left\{ -\frac{\sin(2\phi)}{4\delta_r}, 0, \left(\frac{R}{4\delta_r^2} - \frac{3}{4\delta_r} \right) \times \sin^2 \theta \sin^2 \phi \right\} B_0 v_0^2. \tag{41}$$

The toroidal current increases the most. Since largest gradients are in radial direction, that leads to growth of B_θ, see Eq. (42).

Using Eq. (40), neglecting B_r component (small near the surface, nonpenetrating magnetic field), we find divergent terms

$$B_\theta = \left(-\frac{3R^2}{4(r^3 - R^3)} + \frac{\ln \left(\frac{r^2 + rR + R^2}{(r - R)^2} \right)}{4r} \right) \sin \theta \sin^2 \phi R B_0 v_0^2. \tag{42}$$

The most dominant divergent term is

$$\delta B_\theta = -\frac{R}{4\delta_r} B_0 v_0^2 \sin \theta \sin^2 \phi. \tag{43}$$

Equation (43) gives an estimate of the magnetic field perturbation—hence the justification of the first order expansion. The condition $\delta B_\theta \leqslant B_0$ implies that the first order
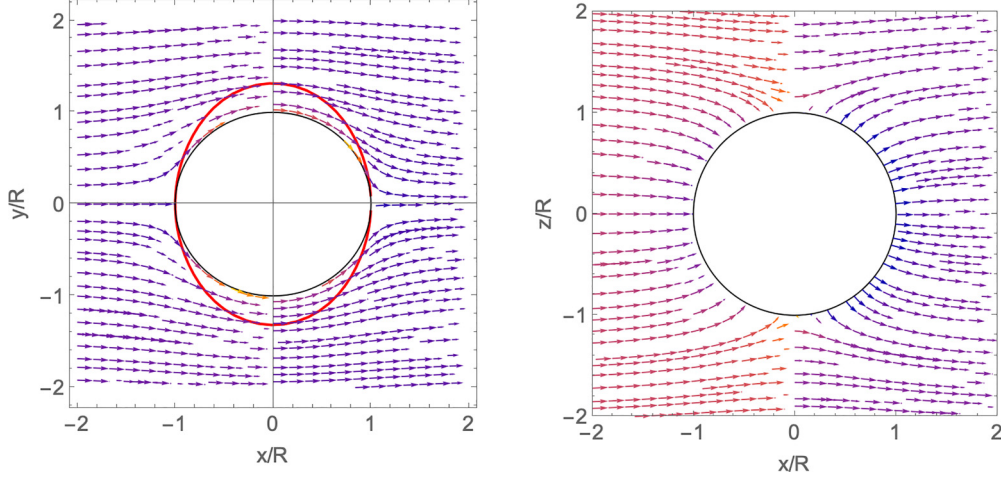
FIG. 5. Flow lines in the $z = 0$ and $y = 0$ plane. A slight disconnection at $x = 0$ is an artifact of the plotting procedure. In the plane $x = 0$ the velocity is $\beta_{EM} = (y^2 + z^2)^{3/4}/\sqrt{(y^2 + z^2)^{3/2} - 1}\, v_0 \mathbf{e}_x$. Red lines indicate regions where $\beta_{EM} \geqslant 1$.

expansion is valid for

$$\frac{\delta_r}{R} \geqslant v_0^2, \tag{44}$$

consistent with Eq. (36).

Thus, both the electric field and the magnetic field diverge on the surface—this is electromagnetic draping. The electric field diverges in linear terms in v_0, magnetic field in v_0^2. The ratio of divergent terms in the first order electric field and second order magnetic field is

$$\frac{E_r}{\delta B_\theta} = -2\sqrt{3}\frac{\sqrt{\delta r/R}}{v_0 \sin\phi}. \tag{45}$$

Thus, the divergent second order term in magnetic field cannot generally compensate for the divergent first order term in electric field.

Next, the longitudinal current

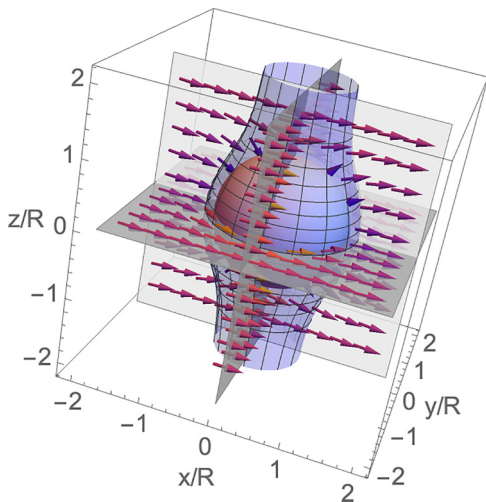$$\mathbf{J}_\parallel = G(r, \theta, \Phi)\mathbf{B}_0 \tag{46}$$

FIG. 6. Velocity plot.

follows from stationary condition

$$\mathrm{div}\,(\mathbf{J}_{EM} + \mathbf{J}_\parallel) = 0. \tag{47}$$

We find

$$\mathrm{div}\,\mathbf{J}_{EM} \approx \left(\frac{1}{\delta_r^2} - 3\frac{1}{R\delta_r}\right)\sin\phi\cos\phi\, v_0^2 B_0. \tag{48}$$

Function G must be $\propto \sin\phi\cos\phi$, and we find

$$\mathrm{div}\,(G\mathbf{B}_0) \approx (2\delta_r\cos\theta\partial_r G - \sin\theta\partial_\theta G)\frac{3}{4}\sin(2\phi)\frac{B_0}{R}. \tag{49}$$

To match θ-independent $\mathrm{div}\,\mathbf{J}_{EM}$ [Eq. (48)] function G should be necessarily divergent either at $\theta = 0$ (the $\partial_\theta G$ term) or at $\theta = \pi/2$ (the $\partial_r G$ term).

IV. DOUBLE MAGNETIZED (ANTI)ALIGNED CASE

Results of the single magnetized neutron star can be generalized to the double magnetized aligned or anti-aligned case in the case when the reconnection effects are not important and the magnetospheres remain topologically disconnected (see Refs. [7,8] for the case when the magnetospheres are strongly coupled). Recall that for a metal ball in external magnetic field, the field is a sum of dipole and external field. For double magnetized case, then the parameter R is the radius where the field of the star matches the external field, see Fig. 7. Equivalently, in expression for $\mathbf{B}_d$, a change $R^3 B_0 \to \mu$ in Eq. (17), the magnetic moment of the star. In the anti-aligned case, when the magnetic moment opposes the external field, there are no currents; in the opposite aligned case there is a toroidal surface current at R.

The location of the boundary between the external magnetic field and that of the neutron star magnetosphere is not fixed now (for single-magnetized case it was the surface of the star). But as we discuss in Appendix A any distortion of the surfaces is second order in v_0. Thus, in the linear regime all the previous derivations for the 1M-DNS case remains valid.
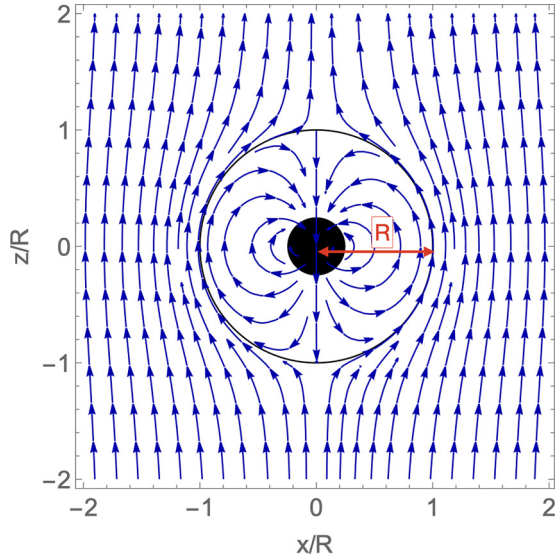
FIG. 7. Double magnetized anti-aligned case. Topologically disconnected intrinsic dipolar field matches the external field at $r = R$. The black circle in the center indicates the neutron star.

V. DISCUSSION

In this paper we argue that effects of electromagnetic draping—creation of dissipative layer near the merging neutron star—may lead to generation of observable precursor emission. The draping effect is well known in space and astrophysical plasmas [20–22]. In the conventional MHD limit, when the electric field is not an independent variable, creation of the magnetized layer (for super-Alfvenic motion) does not lead to dissipation, only breakdown of the weak-field approximation in the draping layer.

We argue that relativistic plasmas are different. In this case the s electric field is an independent dynamic variable; also charge densities are important. As a result, the set of ideal conditions, $\mathbf{B} \cdot \mathbf{E} = 0$ and $B \geqslant E$, is violated. Since the approach we took—expansion in small velocity—involves step-by-step approximation, it is feasible that higher order effects will smooth out the divergencies. We think this is unlikely: divergent first-order electric field is not compensated by the second order magnetic field, see Eq. (45). Instead, the second order magnetic field is divergent on its own. Divergent electric currents, see Eq. (41), will lead to resistive dissipation.

Thus, we expect electromagnetic dissipation near the neutron star (or magnetospheric boundary). Particle will be accelerated and eventually collimated to move that particle along magnetic field lines, see Fig. 8.

The effect of collimation may be important for the detection of precursors, since the expected powers are not very high. The expected powers in the 1M-DNS and 2M-DNS scenarios were discussed by Ref. [4]. If a neutron star is moving in the field of a primary's dipolar magnetic field at orbital separation r, the expected powers is [2,9]

$$L_1 \sim \frac{G B_{NS}^2 M_{NS} R_{NS}^8}{c r^7} = 3 \times 10^{41} (-t)^{-7/4} \text{ erg s}^{-1}, \quad (50)$$

where in the last relations the time to merger t is measured in seconds. (Index 1 indicates here that the interaction is between single magnetized neutron star and unmagnetized one.) Mag-
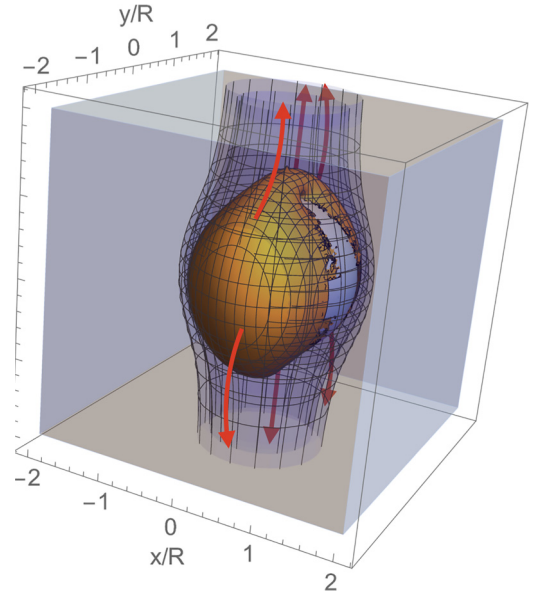

FIG. 8. Expected jets from a neutron star moving through force-free magnetic field. Yellow regions are dissipative regions, $E \geqslant B$. Quasicylindrical surfaces are magnetic flux surfaces. Dissipation within the $E \geqslant B$ regions would produce double-tongue-like jet structures.

netospheric interaction of two magnetized neutron stars can generate larger luminosity than the case of one star moving in the field of the companion [4]. In this case

$$L_2 \sim \frac{B_{NS}^2 G M_{NS} R_{NS}^6}{c r^5} = \frac{c^{21/4} B_{NS}^2 R_{NS}^6}{(-t)^{5/4} (G M_{NS})^{11/4}}$$
$$= 6 \times 10^{42} (-t)^{-5/4} \text{ erg s}^{-1}. \quad (51)$$

(Index 2 indicates here that the interaction is between two magnetized neutron star.) The ratio of luminosities of the models 1M-DNS and 2M-DNS is

$$\frac{L_2}{L_1} = \left(\frac{GM}{c^2 R_{NS}}\right)^{3/2} \sqrt{\frac{(-t)c}{R_{NS}}} \approx 16\sqrt{-t}. \quad (52)$$

Thus L_2 dominates L_1 prior to merger. This is due to larger interaction region, of the order of the magnetospheric radius, instead of the radius of a neutron star.

Qualitatively, for the nonmagnetar magnetic field the power [Eq. (51)] is fairly small. Even at the time of a merger, with $t \sim 10^{-2}$ seconds, the corresponding power is only $L \sim 10^{45}$ erg s^{-1}—hardly observable from cosmological distances by all-sky monitors. The best case is if a fraction of the power [Eq. (51)] is put into radio. If a fraction of η_R of the power is put into radio, the expected signal then is

$$F_R \sim \eta_R \frac{L_2}{4\pi d^2 \nu} \approx 0.1 \text{ Jy } \eta_{R,-5} (-t)^{-5/4}. \quad (53)$$

This is a fairly strong signal that could be detected by modern radio telescopes.

Our results indicate that even in the single magnetized case we expect relativistic jets (or "tongues") produced due to electromagnetic interaction of merging neutron stars, with correspondingly beamed emission pattern. Another way to

produce higher luminosity is at the moments of topological spin-orbital resonances [8].

The data underlying this article will be shared on reasonable request to the corresponding author.

ACKNOWLEDGMENT

APPENDIX A: FIRST ORDER VARIATION OF $\alpha - \beta - \Phi$ ARE VANISHING

Here we demonstrate that in the first order of v_0 the variation of $\alpha - \beta - \Phi$ are vanishing.

Let us expand

$$
\begin{aligned}
\alpha &= \alpha_0 + \epsilon \alpha_1, \\
\beta &= \beta_0 + \epsilon \beta_1, \\
\Phi &= \Phi_0 + \epsilon \Phi_1.
\end{aligned} \tag{A1}
$$

The orthogonality constraint

$$
(\nabla \alpha) \cdot (\nabla \beta) = 0 \rightarrow (\nabla \alpha_0) \cdot (\nabla \beta_1) + (\nabla \alpha_1) \cdot (\nabla \beta_0) = 0 \tag{A2}
$$

implies

$$
\begin{aligned}
\nabla \alpha_1 &= a_1 \nabla \alpha_0 + a_2 \nabla \Phi_0, \\
\nabla \beta_1 &= b_1 \nabla \beta_0 + b_2 \nabla \Phi_0.
\end{aligned} \tag{A3}
$$

On the other hand,

$$
(\nabla \alpha) \cdot (\nabla \Phi) = 0 \rightarrow (\nabla \alpha_0) \cdot (\nabla \Phi_1) + (\nabla \alpha_1) \cdot (\nabla \Phi_0) = 0, \tag{A4}
$$

hence

$$
\begin{aligned}
\nabla \alpha_1 &= a_1 \nabla \alpha_0 + d_2 \nabla \beta_0, \\
\nabla \Phi_1 &= c_1 \nabla \Phi_0 + c_2 \nabla \beta_0.
\end{aligned} \tag{A5}
$$

Thus, to keep all surfaces orthogonal we need

$$
\begin{aligned}
\nabla \alpha_1 &= a_1 \nabla \alpha_0, \\
\nabla \beta_1 &= b_1 \nabla \beta_0, \\
\nabla \Phi_1 &= c_1 \nabla \Phi_0.
\end{aligned} \tag{A6}
$$

Thus, first order perturbations are "locked in".

APPENDIX B: COMPARING ELECTRIC FIELD EQ. (33) WITH OTHER CASES

The electric field Eq. (33) is not too different from the vacuum case, where for electric field along y direction at infinity

$$
\begin{aligned}
\Phi^{(\text{vac})} &= E_0 (1 - (R/r)^3) r \sin \theta \sin \Phi, \\
E_r^{(\text{vac})} &= -(1 + 2R^3/r^3) \sin \theta \sin \Phi E_0, \\
E_\theta^{(\text{vac})} &= (1 - (R/r)^3) r \cos \theta \sin \Phi E_0, \\
E_\phi^{(\text{vac})} &= (1 - (R/r)^3) \cos \Phi,
\end{aligned} \tag{B1}
$$

with surface charge density

$$
\sigma^{(\text{vac})} = \frac{3}{2\pi} \sin \Phi \sin \theta E_0. \tag{B2}
$$

Fields Eqs. (33) and (B1) have the same angular dependence, but different radial dependence. The electric field Eq. (B1) has a nonzero component along B_0:

$$
\mathbf{E}^{(\text{vac})} \cdot \mathbf{B}_0 = \frac{3R^3(r^3 - R^3) \sin(2\theta) \sin \phi}{4r^6} E_0 B_0. \tag{B3}
$$

Another possible approximation, that of an incompressible flow around a sphere with kinematically added magnetic field, with velocity

$$
\begin{aligned}
\mathbf{v}^{(\text{inc})} = \{ &-(1 - R^3/r^3) \sin \theta \cos \phi, -(1 + R^3/(2r^3)) \\
&\times \cos \theta \cos \phi, (1 + R^3/r^3) \sin \phi \} v_0,
\end{aligned} \tag{B4}
$$

would produce electric field with similar angular dependence,

$$
\begin{aligned}
\mathbf{E}^{(\text{inc})} &= -\mathbf{v}^{(\text{inc})} \times \mathbf{B}_0, \\
E_r &= (1 + R^3/(2r^3))^2 \sin \theta \sin \phi \, v_0 B_0, \\
E_\theta &= (1 - R^3/(2r^3) - R^6/(2r^6)) \cos \theta \sin \phi \, v_0 B_0, \\
E_\phi &= (1 - R^3/(2r^3) - R^6/(2r^6)) \cos \phi \, v_0 B_0.
\end{aligned} \tag{B5}
$$

A drawback of this approach is that the electric field has nonzero curl

$$
\nabla \times \mathbf{E}^{(\text{inc})} = \left\{ 0, -\frac{9R^6 \cos \phi}{4r^7}, \frac{9R^6 \cos \theta \sin \phi}{4r^7} \right\} v_0 \mathbf{B}_0, \tag{B6}
$$

and hence cannot be stationary.

[1] B. P. Abbott, R. Abbott, T. D. Abbott, F. Acernese, K. Ackley, C. Adams, T. Adams, P. Addesso, R. X. Adhikari, V. B. Adya *et al.*, Phys. Rev. Lett. **119**, 161101 (2017).

[2] B. M. S. Hansen and M. Lyutikov, Mon. Not. R. Astron. Soc. **322**, 695 (2001).

[3] D. Lai, Astrophys. J. **757**, L3 (2012).

[4] M. Lyutikov, Mon. Not. R. Astron. Soc. **483**, 2766 (2019).

[5] P. Goldreich and D. Lynden-Bell, Astrophys. J. **156**, 59 (1969).

[6] E. Nakar and T. Piran, Nature (London) **478**, 82 (2011).

[7] E. R. Most and A. A. Philippov, Astrophys. J. **893**, L6 (2020).

[8] S. A. Cherkis and M. Lyutikov, Astrophys. J. **923**, 13 (2021).

[9] M. Lyutikov, Phys. Rev. D **83**, 124035 (2011).

[10] M. Lyutikov, Phys. Rev. D **83**, 064001 (2011).

[11] C. Palenzuela, L. Lehner, and S. L. Liebling, Science **329**, 927 (2010).

[12] D. Alic, P. Moesta, L. Rezzolla, O. Zanotti, and J. L. Jaramillo, Astrophys. J. **754**, 36 (2012).

[13] P. Goldreich and W. H. Julian, Astrophys. J. **157**, 869 (1969).

[14] E. T. Scharlemann and R. V. Wagoner, Astrophys. J. **182**, 951 (1973).

[15] V. S. Beskin, *MHD Flows in Compact Astrophysical Objects: Accretion, Winds and Jets* (Springer, Berlin, Heidelberg, 2009).

[16] H. Grad, Phys. Fluids **10**, 137 (1967).

[17] V. D. Shafranov, Rev. Plasma Phys. **2**, 103 (1966).

[18] D. Stern, J. Geophys. Res. **72**, 3995 (1967).

[19] L. D. Landau and E. M. Lifshitz, *The Classical Theory of Fields* (Pergamon Press, Oxford, 1975).

[20] I. H. Cairns, *Physics of the Outer Heliosphere*, edited by V. Florinski, N. V. Pogorelov, and G. P. Zank, AIP Conf. Proc. Series (AIP, New York, 2004), Vol. 719, pp. 381–386.

[21] M. Lyutikov, Mon. Not. R. Astron. Soc. **373**, 73 (2006).

[22] L. J. Dursi and C. Pfrommer, Astrophys. J. **677**, 993 (2008).